Title

Review of Integrated Structured Light Architectures

Author

Petrosian, David

Publication Date

2023-12-11

Review of Integrated Structured Light Architectures

David Petrosian

UCLA, Department of Electrical and Computer Engineering
petroleum@ucla.edu

Abstract

In this review, we will be analyzing a phased-array based laser architecture, which can manipulate lights geometric and topological states, and then calculating the data points on the Poincaré Sphere.

INTRODUCTION

Currently, one way of producing structured light is by using spatial light modulators, which can control the intensity and phase of light in an image or Fourier space. Although spatial light modulators have many applications, they are currently limited by their operational damage threshold, and are unfavorable for ultrashort pulse manipulation. By using tiled phased arrays and incorporating phase, amplitude, polarization, and timing as parameters that can be adjusted using a field programmable logic array for real-time programmability, we have the possibility of seeing great advancements in high-resolution imaging, quantum electrodynamics, optical quantum communications, light control and manipulation, and nonlinear topological and nuclear photonics [1].

METHODS

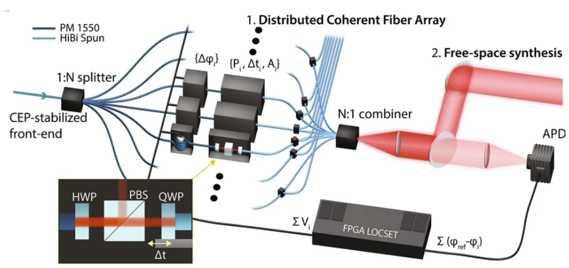

Figure 1: Experimental Design of Laser Architecture

The paper "Integrated Structured Light Architectures" investigates a new laser technology for producing structured light. The motivation behind this study was due to the promising applications of structured photonics, but the lacking technologies that make us unable to exploit more degrees of freedom when generating light with an adaptable structure. The experimental configuration uses a carrier-envelope phase-stabilized front end, meaning that the difference between the optical phase of the carrier wave and the envelope position is minimized. CEP stabilization is essential in order to guarantee pulse-train absolute phase consistency across all beamlines. The signal is then passed through a 1:N beam splitter providing us with N different beamlines. One beamline acts as a reference allowing us to control the inter-beamline phase offset. Using the FGPA, we can phase-lock the other 7 beamlines, by actively manipulating the field parameters. The phase is manipulated by a piezoelectric transducer-based fiber stretcher that allows the user to impose a phase relationship. The intensity and polarization are manipulated by using a half-wave plate (HWP), polarizing beam splitter, and quarter-wave plate (QWP) placed on a fiber pigtailed delay stage. After each parameter has been manipulated, each individual beamline's polarization state is preserved and the beams are transmitted to a N:1 combiner. The composite beam is then synthesized in free space with a micro-lens array in a tiled-aperature configuration with the seven beamlines arranged hexagonally in order to be spatio-temporally overlapped onto an avalanche photodiode.

RESULTS AND INTERPRETATION

This study provides many results in order to substantiate the claim of the effectiveness of their architecture. Some ways that this is done is by detailing the different phase-fronts for near-field configurations, showing the precise control over the relative phase and CEP. It also shows that the architecture has the ability to produce beams with spatially and temporally different spin angular momentum distributions. In order to further interpret this study, I will discuss the calculation of the Poincaré Sphere using Stokes parameters in order to contextualize the geometric representation of the polarization of light. In order to do this we must first do the polarization vector map calculations which are generated from Stokes parameters. Stokes parameters (S_0, S_1, S_2, S_3) are values that describe the state of polarization of light. S_0 represents the total intensity of the optical beam, S_1 represents the difference in intensity between horizontally and vertically polarized light, S_2 represents the difference in intensity between the linear polarization of light at 45° and 135°, and S_3 represents the difference in intensity between R and L circularly polarized light. In order to obtain Stokes parameters we take seven images, one of the full field and one for each of the six projections on the Poincaré Sphere. Each image of size N x M is captured by using a QWP, a have-wave plate, a polarizing beam splitter, and an InGaAs camera [1]. The QWP is a plate of an anisotropic material and a quarter period thickness and it can be used to convert linearly polarized waves to circular or elliptic polarization and back. If the plate instead has a half period thickness, it is a HWP, and can be used to rotate the polarization direction of a linearly polarized wave [2]. After the image is captured, it is then processed to ensure that each image is capturing the same region of the field. This is done by taking a smaller image of n x m from the full image and then calculating the normalized cross-correlation between the smaller image and each projection. Once the cross-correlation reaches its maximum value, the image is then cropped to N x M. Lastly, before using the images to calculate the local Stokes parameters, we must also take a step to remove errors in pixel differences between images. This is done by subdividing the images into n x m macro-pixels, where each contains the mean of a subset of true pixels α x β to where αn = N and βm = M [1]. Based on this we can center and subdivide the images before calculating the Stokes parameters, which can then be found using [4]:

$S_0 = E_{0x}^2 + E_{0y}^2$ | $S_1 = E_{0x}^2 - E_{0y}^2$ | $S_2 = 2E_{0x}E_{0y} - \cos\delta$ | $S_3 = 2E_{0x}E_{0y}\sin\delta$, $\delta = \delta_y - \delta_x$

Once we have found the Stokes parameters, we can then calculate the local polarization ellipse by using these formulas for eccentricity, the tilt relative to a fixed axis, and the chirality respectively [1]:

$$\boldsymbol{e} = \sqrt{\frac{2\sqrt{\boldsymbol{S}_1^2 + \boldsymbol{S}_2^2}}{1 + \sqrt{\boldsymbol{S}_1^2 + \boldsymbol{S}_2^2}}} \qquad 2\boldsymbol{\theta} = \tan^{-1}\frac{\boldsymbol{S}_2}{\boldsymbol{S}_1}$$

Chirality: determined by sign of S_3

Once the polarization ellipse has been obtained, we can take the azimuthal (Ψ) and ellipticity (χ) parameters and map them to angles on our Poincaré Sphere (figure 2) [5]:

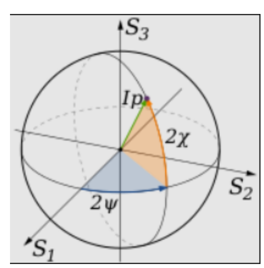

Figure 2: The Poincaré Sphere

The total beam power is usually not of interest so we use a normalized stokes vector by dividing the stokes vector by total intensity leaving us with three significant Stokes parameters (S_1, S_2, S_3). The stokes parameters can then be translated to spherical units by using the formula below in order to plot them on the sphere [6]:

$$S_1 = \cos(2\chi)\cos(2\Psi) \ | \ S_2 = \cos(2\chi)\sin(2\Psi) \ | \ S_3 = \sin(2\chi)$$

Polarization ellipses make calculations for obtaining the new angles of a polarized beam that propagate through one or more polarizing elements very difficult [3]. The Poincaré Sphere provides an ideal representation to perform these calculations. For example, if we consider a setup with an initial polarization angle of 30°, a QWP orientation of 45°, and a HWP orientation of 60°, using the polarization ellipse approach we first calculate the initial state:

$$E = \begin{vmatrix} \cos(30°) \\ \sin(30°) \end{vmatrix} = \begin{vmatrix} \sqrt{3}/2 \\ i/2 \end{vmatrix} \qquad J_{QWP} = \begin{vmatrix} 1 & 0 \\ 0 & i \end{vmatrix} \qquad J_{QWP}E = \begin{vmatrix} \sqrt{3}/2 \\ i/2 \end{vmatrix}$$

$$J_{HWP} = \begin{vmatrix} \cos(2*60°) & \sin(2*60°) \\ \sin(2*60°) & -\cos(2*60°) \end{vmatrix} \qquad J_{HWP}E_{QWP} = \begin{vmatrix} -1/2 & \sqrt{3}/2 \\ \sqrt{3}/2 & i/2 \end{vmatrix} \ \begin{vmatrix} \sqrt{3}/2 \\ i/2 \end{vmatrix}$$

From this point, we can then calculate the final complex vector in order to determine polarization state. However when using the Poincaré Sphere, we find our initial state by placing it on the equator at 60°. Then through the QWP we rotate the point 90° about an axis at 45° from the horizontal. Then through the HWP we rotate the point 180° about an axis at 120°. Then we interpret the final position on the sphere in order to determine its polarization state. In order to validate the results of the paper, we could apply the theoretical values expected onto the Poincaré Sphere, and match the calculated eccentricity, tilt, and chirality against the values expected.

CONCLUSIONS

The architecture presented by the authors of “Integrated structured light architectures” shows that by using tiled phased arrays, and manipulating amplitude, polarization, phase, and timing of the beam, we can generate an almost limitless amount of transverse field configurations, while also offering clear improvements over spatial light modulators. We can also see the effectiveness of using a Poincaré Sphere when analyzing the polarization state of light, and its superiority over polarization ellipses. I believe that one of the next steps in the field is taking advantage of the LOCSET technique’s ability to accommodate active control of hundreds of discrete beamlines in order to be applicable to applications that require a beam that is closer to an ideal case.

REFERENCES

1. Lemons, Randy, et al. "Integrated structured light architectures." Scientific reports 11.1 (2021): 1
2. Liu, J.M. Principles of Photonics. Cambridge University Press, 2016
3. SPIE. (n.d.). “Poincaré Sphere”. https://spie.org/publications/fg05_p10-11_poincare_sphere
4. SPIE. (n.d.). “Stokes Polarization Parameters”. https://spie.org/publications/fg05_p12-14_stokes_polarization_parameters?SSO=1"
5. Wikipedia contributors. (n.d.). “Unpolarized light”. https://en.wikipedia.org/wiki/Unpolarized_light#Poincar%C3%A9_sphere
6. Thorlabs. (n.d.). [Data Points on the Poincaré Sphere section]. https://www.thorlabs.com/newgrouppage9.cfm?objectgroup_id=14200#:~:text=Data%20Points%20on%20the%20Poincar%C3%A9%20Sphere&text=Points%20on%20the%20equator%20correspond,indicate%20other%20elliptical%20polarization%20states.